Analysis of Enamel Erosion Characteristics by Carbonated Soft Drink and Components of Heated Enamel Using micro-FTIR

（micro-FTIR を用いた炭酸飲料によるエナメル質浸食特性と
加熱エナメル質構成要素の解析）

Arata Watanabe

Departments of Histology, Nihon University School of Dentistry at Matsudo

日本大学松戸歯学部

組織学講座

渡辺　新

（指導：岡田裕之　教授）

本論文は

1) Analysis of Heated Enamel Using Micro-FTIR

International Journal of Oral-Medical Sciences 20 (3): 1-6, 2021

2) Second Order Differentiation Analysis of Micro FTIR Method Revealed the Variable Erosion Characteristics of Carbonated Soft Drink for the Individual Human Teeth Enamel

Journal of Hard Tissue Biology 28 (1): 7-12, 2019

をまとめたものである。

1. Abstract

Purposes:

In this study, to clarify how these differences affect each individual, since biological apatite is rich in ion substitution in the crystalline lattice, has many crystalline lattice irregularities, and has low crystallinity compared to synthetic and mineral apatite, which has good crystallinity. Therefore, two analyses were conducted: 1) a simpler method using micro FTIR to analyze the difference in erosive power of enamel immersed in carbonated beverages, and 2) focusing on the individual differences in enamel revealed by the analysis, the materials were powdered, and further heat treated to obtain finer component differences.

Materials and Methods:

This study was conducted with the approval of the Ethics Committee of Nihon University School of Dentistry at Matsudo (Approval No. EC 17-015).

Teeth were cut longitudinally into thin slices at intervals of approximately 0.5 mm, from which a central piece was selected.

1) The inner and outer layers of the micro-FTIR spectroscopic analysis was carried out using the human teeth sections soaking into a carbonated soft drink (Sprite®) for 1 and 7 days. Hereafter, “d1” represented the sample soaking duration of 1 day and “d7” of 7 days. After the twenty human teeth examined, the teeth were grouped into two; the lightly dissolved one and extremely heavily dissolved one based on the macroscopical and microscopical features after the soaking experiment. Among the twenty human teeth samples examined in this study, two typical samples were explained in this study. The sample A was the lightly dissolved one, and the sample B was the heavily dissolved one.

2) Only the enamel was powdered using a mortar. A portion of the powder was suspended in water, spread on Low-E glass slides, air-dried, and analyzed by a micro-FTIR instrument.

Results:

1) The micro-FTIR spectroscopy showed the drastic changes in the P-O absorption bands of the outer layer enamel of both samples, while those of the inner layer enamel remained almost unalterably. This result indicated that the erosive processes mainly attacked the phosphate ion environments in the biological apatite crystal structure of tooth enamel. The second order differential curves of the micro-FTIR patterns firstly reported here showed the small but significant P-O band peak shifts among all analyzing points except for d7 of Sample B, suggesting the individual physicochemical characteristic of tooth enamel apatite.

2) As a result, the analysis pattern before heating showed the common enamel pattern reported by many authors, but the peak values of some absorption bands were different in the samples. Conversely, the analysis pattern after heating indicated several peaks that were not present in the absorption band before heating, and more detailed differences in peak values were observed. After the heating, the PO_4^{3-} absorption band revealed the peak, and the shift of the peak cloud be attributed to the subdivision compared to that before heating. The PO_4^{3-} absorption band, is used to evaluate hydroxyapatite crystallinity, and changes in this band indicate changes in the crystallinity of hydroxyapatite. The CO_3^{2-} absorption bands showed many peak values attributed to B-CO_3^{2-} in the sample before and A-CO_3^{2-} after heating.

Conclusion:

This study found individual differences in the constituents in human enamel biological apatite crystals, suggesting that the compositional variation was amplified by heating. The enamel of individual specimens clearly showed characteristic differences, indicating the diversity of enamel. It was suggested that generally accepted caries protection methods might not be a common standard for every people and every tooth enamels.

2. Introduction

A number of the studies on the caries formation in vivo and in vitro had been reported, but the results of these studies are not concluded, and they have not yet revealed a unified mechanism of the caries progress (1-3). Furthermore, studies on acid erosion have shown that enamel dissolution is inversely proportional to the pH of the beverage, increasing in parallel with the solubility of enamel apatite and having little more effect than Sprite® even when the pH of the juice is as low as Sprite® (4). It should be noted, however, that the biological apatites consisting the human tooth enamel showed the remarkable deviations in their crystallographic characteristics among the portions (5). However, most of the studies that have been conducted have compared enamel from mainly animal teeth, multiple individuals and tooth species, with synthetic apatite and post-demineralized enamel.

Hence, the purpose of this experiment was to compare the effects of soft drinks and individual differences in enamel. Therefore, two analyses were conducted: 1) a simpler method using micro FTIR to analyze the difference in erosive power of enamel immersed in carbonated beverages, and 2) focusing on the individual differences in enamel revealed by the analysis, the materials were powdered, and further heat treated to obtain finer component differences.

Human enamel is a highly crystalline hard tissue composed of about 97 % inorganic and about 3 % organic matter and water. The inorganic material is a type of hydroxyapatite crystal but differs from the theoretical hydroxyapatite in several respects. The substitution of PO_4^{3-} to HPO_4^{2-}, OH^- to CO_3^{2-}, Ca^{2+} to Na^+, Mg^{2+} and other ions has revealed that enamel crystals differ in many physicochemical properties even within an individual tooth (6, 7). Given the above, it is necessary to note the differences in enamel in each individual, and a useful microanalysis method is needed for this analysis. One of the compositional analysis methods that can meet this

requirement is micro-Fourier Transform Infrared Spectroscopy (micro-FTIR). micro-FTIR has been widely used for the chemical characterization of hard tissues in the past decades because it can detect the frequencies of vibrational modes of organic and inorganic molecules, making it an ideal technique for analyzing the chemical structure of natural materials (8, 9). Chemical components such as water or OH^-, phosphate group, carbonate group and collagen component in biological apatite show strong peaks in FTIR patterns, and the most analyzable and representative compounds are phosphate group and carbonate group in hard tissues (10). Studying how these compounds decompose, change and disappear when human enamel is heated to high temperatures will reveal more detailed differences (11). In other words, by analyzing the changes in the heated enamel, one can determine the differences in composition before heating.

3. Materials and Methods

This study was conducted with the approval of the Ethics Committee of Nihon University School of Dentistry at Matsudo (Approval No. EC 17-015).

3-1. Second Order Differentiation Analysis of Micro FTIR Method Revealed the Variable Erosion Characteristics of Carbonated Soft Drink for the Individual Human Teeth Enamel

1) Human Tooth Samples

Twenty human third molar teeth used in this study were those extracted for dental clinical reasons and pooled in purified water. The teeth selected for this experiment were not having caries lesions but having some white and/or brownish spots. Two longitudinal sections, ca. 0.5 mm thick, were cut from the middle part of each teeth using a low-speed diamond saw (IsoMet, Buehler Co. Ltd., Lake Bluff, IL, USA).

These sections adhered onto the microscopic cover glass using a waterproofing bond (TAISUI-BOND-SOKKAN, Bijutsu Shuppan Educational Co. Ltd., Tokyo Japan). Each bonded section was put into separately a plastic mesh bag and soaked into a 1.5 L carbonated soft drink bottle, Sprite® (Coca-Cola (Japan) Co. Ltd., Tokyo Japan) for the duration periods of 1 day and 7 days (4). Hereafter, “d1” represented the sample soaking duration of 1 day and “d7” of 7 days. After the soaking, these samples were washed in distilled water and kept in a desiccator.

The soaked teeth were grouped into two; the lightly dissolved one and extremely heavily dissolved one on the basis of the macroscopical and microscopical features after the soaking experiment according to the preceding experiment. Among the twenty human teeth samples examined in this study, two typical samples were explained in this study. The sample A was the lightly dissolved one, and the sample B was the heavily dissolved one (12).

2) Microscopic Observation

The samples before and after the soaking experiment were observed and photographed using a stereomicroscope (Leica M60®, and Leica DFC295®; Wetzlar, Germany).

3) Micro Fourier Transform Infrared Spectroscopy (micro-FTIR)

Infrared spectroscopy is one of the oldest and well established experimental techniques for the analysis of not only organic but also inorganic substances. It is convenient, non-destructive, requires less sample preparation, and can be used under a wide variety of conditions (8,9).

The outer and inner parts of the sample A and B were analyzed by means of the micro-FTIR, especially the shift of peak position. The micro-FTIR measurement was carried out at the ST Japan Lab, and the limited number of analyses was done for the samples after the soaking experiment. A micro-FTIR instrument (Survey IR®; Czitek, CT, USA equipped with a Nicolet iS5 FT-IR®; Thermo Scientific, Yokohama, Japan) was used in this study.

Micro-FTIR analysis was carried out under the conditions as follows: Infrared measurement: Reflection mode, Wavenumber range: 350–7,800 cm^{-1}, Detector: DLaTGS/KBr window, Aperture diameter: 100 μm, Resolution ability: 0.8 cm^{-1}, Gain: AUTO, Cumulated number: 64 times.

FTIR spectra analysis software was Panorama Ver4.0 Analytical Software (LabCognition Analytical Software GmbH & Co. KG.). The second differential curve was used to detect the precise peak position as a useful technique in FTIR analysis.

3-2. Analysis of Heated Enamel Using Micro-FTIR

1) Human Tooth Samples

Six human third molars were selected from the extracted teeth stored in the Department of Histology of our university and were judged by gross examination to be

sound without caries or filling material. Teeth were cut longitudinally into thin slices at intervals of about 0.5 mm using a low-speed diamond saw (Buehler Co. Ltd., USA), and five or six whole sections were prepared. The center one was selected from these, and only the enamel was powdered using an agate mortar. The powder was partially suspended in water, spread on Low-E glass slides, air-dried, and analyzed by a micro-FTIR instrument (12). Low-E glass slides reflect more than 95% of near-infrared and infrared light and were used for observation of samples using transmitted light from a microscope.

2) Micro Fourier Transform Infrared Spectroscopy (micro-FTIR)

The compositional analysis by micro-FTIR was performed using a micro-FTIR instrument (Survey IR®; Czitek, CT, USA attached to Nicolet iS5 FT-IR®; Thermo Scientific, Yokohama, Japan) under the following measurement and analysis conditions. Infrared measurement: Reflection mode, Wavenumber range: 350–7,800 cm^{-1}, Detector: DLaTGS/KBr window, Aperture diameter: 100 μm, Resolution ability: 0.8 cm^{-1}, Gain: AUTO, Cumulated number: 64 times. a micro-FTIR instrument analysis was performed before and after heating. This study mainly observed the change in the waveform of PO_4^{3-} and CO_3^{2-} absorption bands.

3) Thermal decomposition

Heat treatment was performed using a RIGAKU TAS-100 DTA/TG simultaneous analyzer with 10–15 mg sample volume. The powdered sample was placed on a platinum plate, and the temperature was raised to 1,000 °C at a rate of 10 °C/min. After heating, the specimens were removed from the furnace and cooled naturally to room temperature in air (11,13)

4. Results

4-1. Second Order Differentiation Analysis of Micro FTIR Method Revealed the Variable Erosion Characteristics of Carbonated Soft Drink for the Individual Human Teeth Enamel

1) Microscopic Observation

The results of the soaking in Sprite® experiments showed unexpectedly wide variations. Among the twenty samples used in this study, only two extreme samples were reported here, because it was sufficient to show the typical variety of the reaction observed.

Fig. 1-1 showed the photographs of the lightly dissolved sample A and the heavily dissolved sample B: after the Sprite® soaking of 1 day and 7 days duration, together with the micro-FTIR analyzing points. Sample A showed many white and brownish coloring spots were observed in all sections. After the soaking of 1 day and 7 days, Sample A's Hunter-Schreger bands were observed remarkably, indicating the sections were subjected strongly the etching effect of the soaking, but the outline of the tooth enamel remained as it was. Sample B showed also many white and brownish coloring spots were observed in all sections. Sample B's Hunter-Schreger bands were more clearly observed in the section after the 7 days soaking, while not so clear in the section after 1 day soaking. The different etching aspects between the samples A and B may be due to the individual variety of the enamel properties. After the 7 days soaking, the outline of the tooth enamel was greatly changed, and the portions of the central fissure and the cusps were dissolved extensively. The thickness of the sample B enamel decreases appreciably.

Comparing the samples A and B, while the erosive power was the same among the experiments, the subjected effects were greatly different, indicating the individual variety of the tooth enamel sensitivity to the acidic attack.

2) Micro Fourier Transform Infrared Spectroscopy (micro-FTIR)

Fig. 1-2 showed the micro-FTIR spectra obtained from the outer and inner tooth enamel portions of the samples A and B, after the Sprite® soaking of 1 day and 7 days duration. In Fig. 1-2, all the spectra of samples A d1 and B d1, and both the outer and inner layers showed the similar pattern holistically and showed the main absorption bands at from 1,100 cm^{-1} to 1,200 cm^{-1}, assigned as of the P-O vibrations in the enamel apatite crystallites. The minor differences of these absorption band patterns at from 1,100 cm^{-1} to 1,200 cm^{-1} and from 500 cm^{-1} to 600 cm^{-1} (Fig. 1-2) reflected the small environmental differences of the P-O tetrahedra and which has been extensively used to monitor the crystallinity of hydroxyapatite. The details of these configurations were not analyzed in this study, because the reflection-mode used was not sufficient to analyze these detailed structural changes. The absorption bands from 1,300 cm^{-1} to 1,500 cm^{-1} due to the B-type CO_2 in the biological apatite were observed in this study, but these bands were too weak to analyze. Therefore, the analysis for these CO_2 were not carried out in this study. After the 7 days soaking the spectra of Sample A (Fig. 1-2 A d7) and the spectra of Sample B outer layer (Fig. 1-2 B d7) showed no significant P-O absorption bands from 1,100 cm^{-1} to 1,200 cm^{-1} at all, while these P-O bands appreciably remained in the inner layers of the sample B d7. These results indicated that the surface layers of the samples A and B tooth enamel were high sensitivity to the acid attack comparing to the inner layers.

Fig. 1-3 showed the second order differential curves obtained from the micro-FTIR patterns. The second order differential curves were usually calculated to detect the peak positions. The peak positions found in this study were listed in Table 1-1. The peak positions represented in the second order differential curves of the sample A, 1,115–1,127 cm^{-1}, were almost the same within the accuracy of the instrument. These absorption band peaks were assigned as *v3* P-O vibrations of hydroxyapatite (900–1,220

cm^{-1}). The sample B s d7 did not show appreciable peaks in the second order differential curves, and sample B d7 outer layer showed the peak shifted. The lost and the peak shift of P-O absorption band suggested the undergoing structural destruction of phosphate molecules of these enamel apatite.

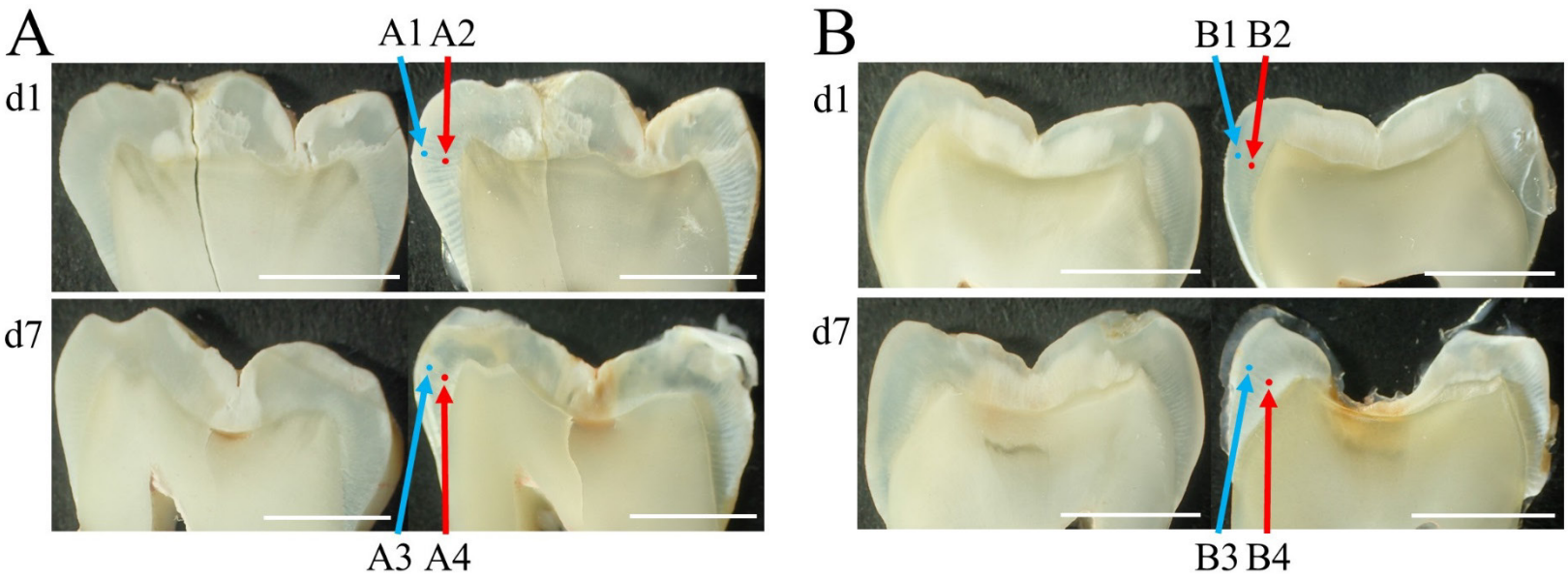

Fig. 1-1 The photographs showing samples A and B: before (Left) and after (Right) the Sprite® soaking of 1 day (d1: Top) and 7 days (d7: Bottom) duration. The arrows and the numbers indicate the micro-FTIR analyzed regions. Scale bars = 5 mm.

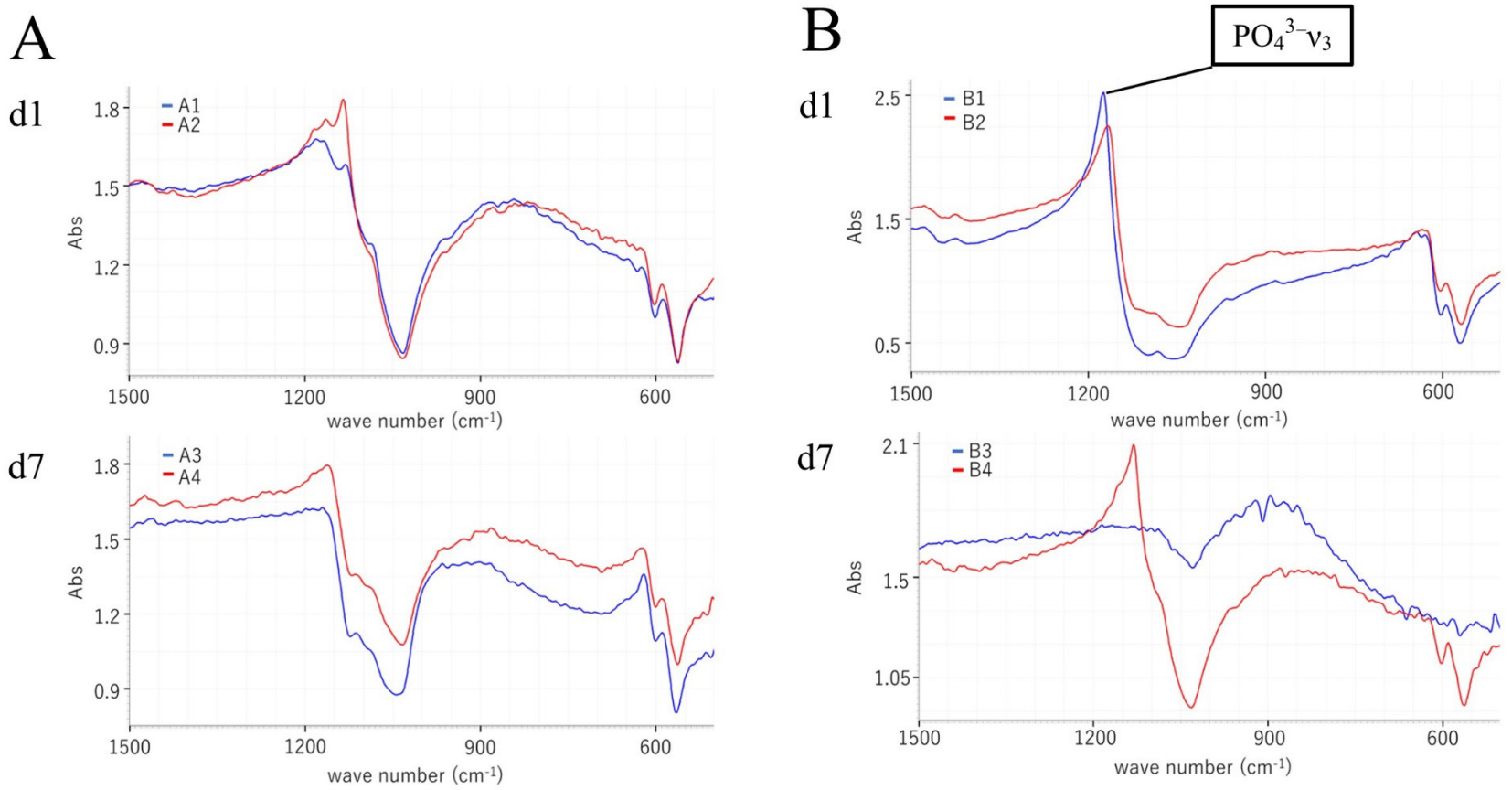

Fig. 1-2 Micro-FTIR patterns, from 500 cm^{-1} to 1,500 cm^{-1}, of the Samples A and B: the soaking of 1 day (d1: Top) and 7 days (d7: Bottom) duration. The blue lines are the spectra from the outer enamel and the red lines from the inner enamel.

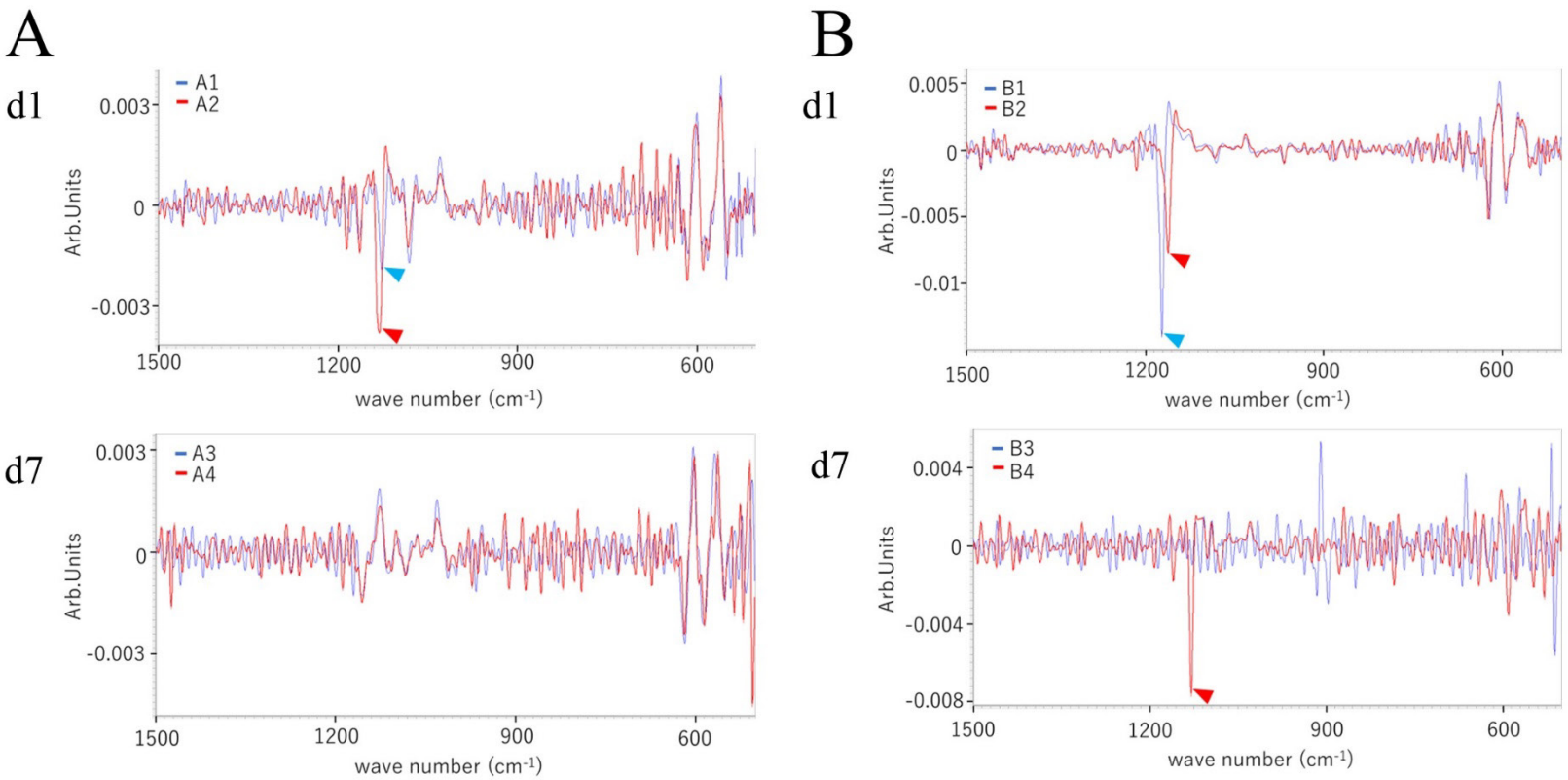

Fig. 1-3 Second order differential curves for the micro-FTIR patterns, from 500 cm^{-1} to 1,500 cm^{-1}, of the Samples A and B: the soaking of 1 day (d1: Top) and 7 days (d7: Bottom) duration. The blue arrowheads indicating the spectra from the outer enamel peak and red arrowheads from the inner enamel.

Table 1-1. The P-O absorption band peaks derived from the second order differential curves. d1: 1 day duration, and d7: 7 days duration. (wavenumber, cm^{-1})

Sample A (lightly dissolved)				Sample B (heavily dissolved)				Hydroxyapatite	
Outer		Inner		Outer		Inner		Reference	Chemical components
d1	d7	d1	d7	d1	d7	d1	d7		
n.d.	*n.d.*	*n.d.*	*n.d.*	*n.d.*	910	*n.d.*	*n.d.*		
1115	1127	1120	1127	*n.d.*	*n.d.*	*n.d.*	*n.d.*	900–1220*	$PO_4^{3-}\nu_3$
1130	1130	1130	1130	1160	*n.d.*	1148	*n.d.*		

*: Lopes, et al.[10)]

4-2. Analysis of Heated Enamel Using Micro-FTIR

The micro-FTIR analysis pattern is shown (Fig. 2-1). In samples A through F, the analysis pattern before heating showed the common enamel pattern reported by many, but differences were observed in the peak values of some absorption bands. Conversely, the absorption band after heating showed several peak values that were not found in the absorption band before heating, and more detailed differences in peak values were observed. The peak values are shown (Table 2-1).

1) Absorption bands of PO_4^{3-}

After heating, the PO_4^{3-} absorption band revealed the peak and the shift of the peak cloud be attributed to the subdivision compared to that before heating. The intensity of the absorption band around 470 cm^{-1} increased after heating compared to before firing, with a peak value of 471 cm^{-1} in samples A, B and C, and a peak value of 474 cm^{-1} in samples D, E and F. The absorption bands around 520–650 cm^{-1} showed peak values of 559 cm^{-1} and 602 cm^{-1} for all samples before heating, 555 cm^{-1} and 598 cm^{-1} for samples A and F after heating, and 548 cm^{-1} and 594 cm^{-1} for sample C. Furthermore, the absorption bands around 1,000–1,100 cm^{-1} were subdivided into peaks after heating. Differences in peak values were observed in each sample. The peaks around 984 cm^{-1} were found in samples A, B, C, D and F after heating, and the peaks around 1,011 cm^{-1} were found in A, B, D, E and F. The HPO_4^{2-} peak of around 1,080 cm^{-1} was detected in all the heated samples.

2) Absorption bands of CO_3^{2-}

The $CO_3^{2-}\nu_2$ absorption band around 860 cm^{-1} to 890 cm^{-1} showed a peak value of 872 cm^{-1} in samples A, B, D, and F before heating, a peak value of 879 cm^{-1} in samples B, D and E after heating, and a peak value of 876 cm^{-1} in the other samples. The peak value at 872 cm^{-1} corresponds to B-CO_3^{2-} and the peak value at 879 cm^{-1} corresponds to A-CO_3^{2-}.

3) Other absorption bands

Before heating, the peak values due to CO_2 adsorption were observed at 2,341 cm^{-1} and 2,360 cm^{-1}. Furthermore, a peak value of 3,572 cm^{-1} due to OH^- was detected in all samples, and the strength increased after heating compared to before heating.

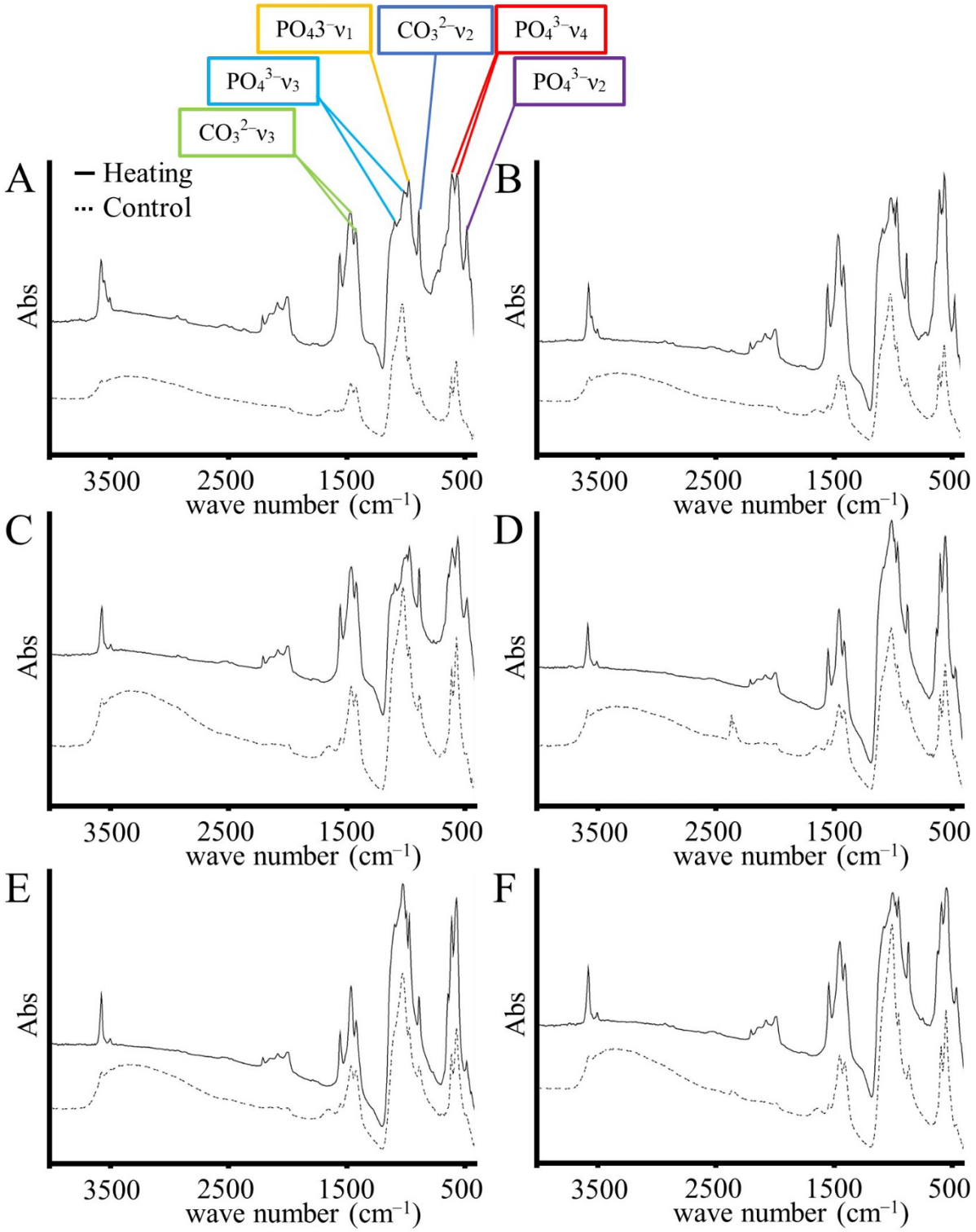

Fig. 2-1 Micro-FTIR patterns, from 500 cm^{-1} to 3,500 cm^{-1}, of the Samples A-F. The analysis pattern before heating showed the common enamel pattern as reported by many authors, but the peak values of some absorption bands differed in the samples. On the other hand, the analysis pattern after heating indicated several peaks that were not present in the absorption band before heating, and more detailed differences in peak values were observed.

Table 2-1 Absorption band peaks. (wavenumber, cm^{-1})

Chemical components	Control						Heating						Reference
	A	B	C	D	E	F	A	B	C	D	E	F	
$PO_4^{3-}\nu_2$							471	471	471	474	474	474	470*
$PO_4^{3-}\nu_4$	559 602	559 602	559 602	559 602	559 602	559 602	555 598	559 602	548 594	559 602	559 602	555 598	520–650*
$CO_3^{2-}\nu_2$	872	872	876	872	876	872	876	879	876	879	879	876	860–890*
$PO_4^{3-}\nu_1$	960	960	960	960	960	960	960	960	960	960	960	960	960*
$PO_4^{3-}\nu_3$	1018	1014	1014	1014	1018	1014	987 1003 1080	984 1011 1080	984 1080	 1011 1080	984 1018 1084	984 1011 1084	900–1220*
$CO_3^{2-}\nu_3$	1412 1454 1547	1412 1454 1547	1412 1454 1547	1412 1454 1547	1412 1454 1543	1412 1454 1543	1412 1458 1547	1412 1458 1547	1412 1454 1547	1412 1454 1547	1412 1454 1547	1412 1454 1547	1350–1520* 1540*
CO_2				2341 2360		2341 2360							2340**
OH^-	3572	3572	3572	3572	3572	3572	3572	3572	3572	3572	3572	3572	3570*

*: Lopes, et al.[10], **: Holcomb, et al.[11]

Green: The PO43- absorption bands after heating. Blue: B-CO_3^{2-}. Red: A-CO_3^{2-}.

5. Discussion

This study is one of the few studies analyzing dental enamel by micro-FTIR, not by normal FTIR. This is the first example of tooth enamel erosion studies. In the field of hard tissue mineralization and demineralization, a few investigations were carried out using FTIR, and various properties of biological apatite crystals have been clarified (10). FTIR analysis is an extremely effective method for examining the state and arrangement of carbonate ions in biological apatite crystals. On the contrary, the study of a phosphate salt in hard tissues have been advanced greatly by FTIR; there was a long debate history about the presence and their site of the carbonate ions in the biological apatite crystal structure (14). It is now well known that hydroxyapatite has a stoichiometric composition, a Ca-deficient composition, and a biological apatite composition. Biological has Mg^{2+}, Na^{+}, K^{+}, etc. in the Ca^{2+} position, HPO_4^{2-}, CO_3^{2-}, etc. in the PO_4^{3-} position, and CO_3^{2-}, F^{-}, etc. in the OH^{-} position as substitution elements in the stoichiometric composition $Ca_{10}(PO_4)_6(OH)_2$ (15). Moreover, it may be noteworthy that enamel carbonate levels influence caries-susceptibility (16).

Studies conducted to determine the intensity of demineralization, have shown that among many carbonated beverages, Sprite® has the highest enamel solubility. The Hunter-Schreger bands were observed more clearly in the highly soluble samples than in the less soluble samples. The clarified Hunter-Schreger bands may be due to preferential demineralization of the acid-sensitive portions of the enamel. Although this result was obtained using Sprite® in the prudent study, it is expected that the use of stronger acids may destroy the structure and make the changes caused by demineralization less noticeable. Therefore, we analyzed the difference in erosive strength of enamel soaked in carbonated beverages using a simpler method using micro FTIR. The samples were not pulverized to simplify the analysis of specific areas. Because of this, some of the analyzed patterns were too weak in intensity to be analyzed

for C-O. Hence, the detection of peaks by second-order derivative curves. Micro-FTIR instrument usually has a potential to analyze an extremely limited region of the object as small as 10 micron-meter square. Applying this micro-analysis technique in this study, the differences of the P-O absorption bands in the FTIR patterns among the tooth enamel samples, not only between the duration periods but also between the portions of the tooth enamel, were obtained. The differences among the portions and between the samples indicated the biodiversity in tooth enamel could not be ignored. Therefore, in order to obtain more detailed component differences, the materials were powdered, heat treated, and analyzed using micro-FTIR. Analyzing the changes in the heated enamel, one can determine the differences in composition before heating. Consequently, the differences in the peak values before and after heating were compared, and detailed differences could be detected by firing. In the study conducted to examine the strength of demineralization, 20 samples were used and only the two extreme samples were reported, because they showed great variability. Therefore, in the study conducted to examine individual enamel variation, the number of samples was reduced, and six samples were studied.

PO_4^{3-} has four vibrational modes, ν_1, ν_2, ν_3 and ν_4, which are the main absorption bands detected in hydroxyapatite. The absorption band of ν_3, which has the strongest peak intensity, is located at about 1,046 cm^{-1}, and the absorption band of ν_3 is observed to overlap the absorption band of ν_1. The absorption band of ν1 is found at 960 cm^{-1}. The absorption band of ν_4 is present in the 520–660 cm^{-1} region, showing a clear and sharp absorption band. Finally, the absorption band of ν_2 is weak in intensity and is located in the region of 470 cm^{-1}. The PO_4^{3-} absorption band is used to evaluate the crystallinity of hydroxyapatite, and changes in this band indicate changes in the crystallinity of hydroxyapatite (17,18). HPO_4^{2-} decreases rapidly between 200 °C and 300 °C, which is thought to affect the crystal size. Additionally, pyrophosphoric acid is

formed in parallel with the decomposition of HPO_4^{2-} when heated above 500 °C. Pyrophosphoric acid was confirmed by X-ray diffraction, and no pyrophosphoric acid was found in the sample heated at 400 °C. At 600 °C, both β- and γ-types were present, and at 800 °C, β-types were found, but γ-types were almost absent (11). Although the presence of pyrophosphoric could not be confirmed in this study because X-ray diffraction was not performed, it was suggested that HPO_4^{2-} may have been incorporated into or adsorbed on apatite in the heated samples. However, these band changes are not due to HPO_4^{2-} alone, but also to the involvement of CO_3^{2-} substitution.

In contrast, CO_3^{2-} has four vibrational modes, of which three absorption bands, ν_2, ν_3 and ν_4, can be observed. The ν_4 absorption band is rarely seen and is of very low intensity. The absorption band of ν_3 is in the 1,300–1,650 cm^{-1} region, and the peak at 873 cm^{-1} is the absorption band of ν_2. The absorption band of ν_3 is assigned to CO_3^{2-} on the surface, not in the lattice of PO_4^{3-} (10,17). In addition, biological apatite has B-site substitution (B-CO_3^{2-}), where CO_3^{2-} is substituted at the PO_4^{3-} position, and A-site substitution (A-CO_3^{2-}), where CO_3^{2-} is substituted at the OH^- position (19). The B-CO_3^{2-} content begins to decrease below 100 °C and disappears at 1,000 °C. The A-CO_3^{2-} content decreases up to 200 °C and increases between 400 °C and 800 °C. The B-CO_3^{2-} molecule is partially converted to A-CO_3^{2-} via CO_2, and the absorption band of CO_2 is known to exist around 2,340 cm^{-1} (11,13). The type and degree of this substitution affect the size and shape, called crystallinity, and the deformation of the crystalline lattice increases the solubility of the crystal, resulting in less stable phases easily soluble in acid (10,20,21). These results suggest a difference in properties between samples in which substitution occurred and those in which it did not. This difference may affect the strength of the demineralization effect. The $CO_3^{2-}\nu_3$ absorption bands showed the same peak values in almost all samples, but some of the peaks were shifted in some samples. Since $CO_3^{2-}\nu_3$ is a carbonate ion on the PO_4^{3-} lattice surface, it

was determined to represent a slight environmental difference.

The absorption bands at 2,341 cm^{-1} and 2,360 cm^{-1} due to CO_2 adsorption result from the transfer of most of the B-CO_3^{2-} to A-CO_3^{2-} via CO_2 (13). In addition, the increase in the intensity of the OH^- peak at 3,572 cm^{-1} was attributed to CO_3^{2-} decomposition, which occurs when enamel is heated, and the reaction with H_2O to produce OH^- (11).

6. Conclusion

This study found individual differences in the constituents in human enamel biological apatite crystals, suggesting that the compositional variation was amplified by heating. The enamel of individual specimens clearly showed characteristic differences, indicating the diversity of enamel. It is necessary to analyze the results using an X-ray diffraction system, to clarify the differences more precisely from a crystallographic point of view.

7. References

1. Roopa KB, Pathak S, Poornima P, Neena IE: White spot lesions: A literature review. J Pediatr Dent, 3: 1-7, 2015.
2. Featherstone JD: Dental caries: A dynamic disease process. Aust Dent J, 53: 286-291, 2008.
3. LeGeros RZ: Chemical and crystallographic events in the caries process. J Dent Res, 69: 567-574, 1990.
4. Larsen MJ, Nyvad B: Enamel erosion by some soft drinks and orange juices relative to their pH, buffering effect and contents of calcium phosphate. Caries Res, 33: 81-87, 1999.
5. LeGeros RZ, Sakae T, Bautista C, Retino M, LeGeros JP: Magnesium and

carbonate in enamel and synthetic apatites. Adv Dent Res, 10: 225-231, 1996.

6. Sakae T, Okuda A: Crystallographical analysis of tooth enamel using milligram samples. J Ultra Res, 91: 77-81, 1985.
7. Boskey A, Imbert L: Bone quality changes associated with aging and disease: a review. Ann N Y Acad Sci, 1410: 93-106, 2017.
8. Andrew CKA, Kazarian SG: Attenuated total reflection fourier-transform infrared (ATR-FTIR) imaging of tissues and live cells. Chem Soc Rev, 45: 1850-1864, 2016.
9. Rey C, Collins B, Goehl T, Dickson IR, Glimcher MJ: The carbonate environment in bone mineral: A resolution-enhanced fourier transform infrared spectroscopy study. Calcif Tissue Int, 45: 157-164, 1989.
10. Lopes CCA, Limirio PHJO, Novais VR, Dechichi P: Fourier transform infrared spectroscopy (FTIR) application chemical characterization of enamel, dentin and bone. Appl Spectrosc Rev, 53: 747-769, 2018.
11. Holcomb DW, Young RA: Thermal decomposition of human tooth enamel. Calcif Tissue Int, 31: 189-201, 1980.
12. Gotouda H, Nasu I, Kono T, Ootani Y, Kanno T, Tamamura R, Kuwada-Kusunose T, Suzuki K, Hirayama T, Hirayama T, Sakae T and Okada H: Erosion by an Acidic Soft Drink of Human Molar Teeth Assessed by X-Ray Diffraction Analysis. J Hard Tissue Biol, 26: 81- 86, 2017.
13. Bachmann L, Diebolder R, Hibst R, Zezell DM: Infrared absorption bands of enamel and dentin tissues from human and bovine teeth. Appl Spectrosc Rev, 38: 1-14, 2003.
14. Sakae T, Nakada H, LeGeros JP: Historical review of biological apatite crystallography. J Hard Tissue Biol, 24: 111-122, 2015.
15. Sakae T, Yanaka S, Watanabe H, Kozowa Y: Formation of porous and dense calcium phosphate structure by cintering of dentin. Nihon Univ J Oral Sci, 22: 45-

51, 1996. (in Japanese)

16. Sa Y, Liang S, Ma X, Lu S, Wang Z, Jiang T, Wang Y: Compositional, structural and mechanical comparisons of normal enamel and hypomaturation enamel. Acta Biomater, 10: 5169-5177, 2014.
17. Rehman I, Bonfield W: Characterization of hydroxyapatite and carbonated apatite by photo acoustic FTIR spectroscopy. J Mater Sci Mater Med, 8: 1-4, 1997.
18. Sakae T: Diversity and university of recent and fossil dental enamel crystallites: and the often seen misunderstandings. J Fossil Res, 43: 72-79, 2011. (in Japanese)
19. Mayer I, Schneider S, Sydney-Zax M, Deutsch D: Thermal decomposition of developing enamel. Calcif Tissue Int, 46: 254-257, 1990.
20. Paschalis EP, Gamsjaeger S, Klaushofer K: Vibrational spectroscopic techniques to assess bone quality. Osteoporos Int, 28: 2275-2291, 2017.
21. Mcelderry JD, Zhu P, Mroue KH, Xu J, Pavan B, Fang M, Zhao G, McNerny E, Kohn DH, Franceshi RT, Holl MMB, Tecklenburg MMJ, Romamoorthy A, Morris MD: Crystallinity and compositional changes in carbonated apatites: Evidence from ^{31}P solid-state NMR, Raman, and AFM analysis. J Solid State Chem, 206: 192-198, 2013.